

Synergistic effect of ionic liquid and methylammonium chloride in crystallization of hybrid haloplumbate for perovskite solar cells

Natalia N. Udalova,^{†,a} Andrey A. Petrov,^{†,b,a} Elizaveta M. Nemygina,^a Karina R. Plukchi,^a Eugene A. Goodilin^{a,c} and Alexey B. Tarasov^{*a,c}

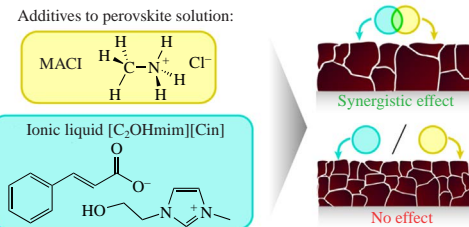
^a Department of Materials Science, M. V. Lomonosov Moscow State University, 119991 Moscow, Russian Federation. E-mail: alexey.bor.tarasov@gmail.com

^b Department of Materials Science, MSU-BIT University, 517182 Shenzhen, China

^c Department of Chemistry, M. V. Lomonosov Moscow State University, 119991 Moscow, Russian Federation

DOI: 10.1016/j.mencom.2024.10.023

The synergistic effect of ionic liquid 1-(2-hydroxyethyl)-3-methyl-1*H*-imidazol-3-ium cinnamate and methylammonium chloride (MACl) on the functional properties of mixed hybrid perovskites was discovered for the first time, which leads to a notable improvement in the quality of perovskite films and the photothermal stability of perovskite solar cells compared to reference devices.



Keywords: perovskite solar cells, hybrid perovskites, ionic liquids, methylammonium chloride, synergistic effect, passivation.

Perovskite solar cells (PSCs) are recognized as the most promising photovoltaic technology with record power conversion efficiency (PCE) exceeding 26%.¹ However, the fabrication of high-efficiency devices with high long-term stability still remains a significant challenge due to intrinsic defects formed in the bulk phase and at grain boundaries in the perovskite film during its crystallization.² The most promising approach to improve the quality of polycrystalline perovskite films is the use of various additives to the perovskite solution as defect passivators.^{3,4} In a wide range of additives, ionic liquids (ILs) have attracted much attention due to the significant improvement in the efficiency and long-term operational stability of PSCs they provide. Recently published comprehensive reviews^{5–10} summarize a large number of different ILs introduced into the precursor solution and their effects on the efficiency and stability of PSCs. Although ILs are generally considered to regulate the crystallization kinetics of perovskite layer and passivate grain boundary defects,¹¹ the mechanism of their influence still remains largely underexplored, requiring further research to develop new ILs with different functional groups.⁷

Until now, the most widely used type of ILs for passivation of perovskite films is 1,3-dialkylimidazolium-based ILs, usually with halide anions.⁷ Indeed, such ILs significantly improve the efficiency and stability of devices. However, it has been shown that due to the inaccessibility of the lone pair of electrons on the N atom in the imidazolium ring of ILs, they cannot eliminate one of the most common and detrimental defects, namely, undercoordinated Pb²⁺ ions on the perovskite surface and grain boundaries.¹² At the same time, it is known that passivators with carboxyl functional groups such as oleic,¹³ pyridinedicarboxylic¹⁴ and 2-thiophenecarboxylic¹⁵ acids can effectively cope with both such defects and halide vacancies.^{16,17} In 2023, Fei *et al.*

showed that carboxyl-functionalized cations in ILs with higher coordination affinity to Pb²⁺ exhibited suppression of nonradiative recombination and higher defect passivation efficiency in perovskite films compared with ILs without carboxyl functional group, resulting in superior long-term stability as well as high efficiency of the fabricated PSCs.¹⁸

Methylammonium chloride (MACl) is another additive frequently introduced into perovskite solutions. MACl is a more volatile compound compared to other components of the perovskite precursor solution and plays a special role in promoting crystallization and grain enlargement of the perovskite.¹⁹ The specific effect of MACl has been demonstrated in the case of formamidinium (FA)-based perovskites, where it stabilizes the α -FA PbI_3 phase during its crystallization, providing overall film stability.²⁰ MACl additive has also been shown to play a distinctive role in manipulating perovskite orientation through the formation of intermediates with PbI_2 , such as $\text{MA}_2(\text{DMF})_2\text{Pb}_3\text{I}_8$.²¹ While MACl has become an indispensable ingredient for the fabrication of FA-based perovskites,²² its effect is often neglected, especially when other additives such as ILs are used.^{23,24} However, it has recently been shown that the simultaneous addition of MACl and IL 1,3-bis(cyanomethyl)-imidazolium chloride can exert a synergistic effect in enhancing the efficiency and stability of PSCs by increasing the crystallinity and degree of orientation of the perovskite film along the [110] crystallographic direction, suppressing unwanted intermediate phases, reducing the defect concentration and improving the phase distribution homogeneity.²⁵

In this work, the passivation effect of IL 1-(2-hydroxyethyl)-3-methyl-1*H*-imidazol-3-ium cinnamate ($[\text{C}_2\text{OHmim}][\text{Cin}]$), containing a carboxyl-functionalized anion, on the functional properties of perovskite films as well as the efficiency and stability of the fabricated solar cells was investigated for the first time. Particular attention was paid to the effect of simultaneous

[†] These authors contributed equally.

addition of IL together with MACl , which was found to promote the enlargement of perovskite grains, enhancement of photoluminescence (PL) intensity and remarkable improvement of the operational stability of both perovskite films and PSCs.

To study the effect of IL on the properties of perovskite films, the $\text{FA}_{0.85}\text{Cs}_{0.15}\text{PbI}_3$ composition was initially chosen because it is one of the most promising compounds for devices with high long-term stability.^{26–28} Thin films of $\text{FA}_{0.85}\text{Cs}_{0.15}\text{PbI}_3$ were fabricated[†] by spin-coating a solution of mixed components in *N,N*-dimethylformamide (DMF) – dimethyl sulfoxide using chlorobenzene as an antisolvent. Additionally, either 0.5 or 1% of IL [$\text{C}_2\text{OHmim}][\text{Cin}]$ and/or 15% of MACl were added to the perovskite solution, *i.e.*, in amounts that correspond to typical concentrations of these additives reported in the literature to stabilize the perovskite phase and achieve the best film quality.

According to scanning electron microscopy (SEM) data, only 15% MACl additive does not contribute to the grain size increase in $\text{FA}_{0.85}\text{Cs}_{0.15}\text{PbI}_3$ films, in contrast to the effects previously observed for pure FAPbI_3 film²⁰ and films of the $(\text{FAPbI}_3)_{0.85}(\text{MAPbBr}_3)_{0.15}$ compositions.²⁹ Addition of only 0.5% [$\text{C}_2\text{OHmim}][\text{Cin}]$ to the precursor solution leads to a 20% increase in grain size, while simultaneous addition of both [$\text{C}_2\text{OHmim}][\text{Cin}]$ and MACl results in a 55% increase in the perovskite grain size, reaching an average size of 305 nm [Figure 1(a)–(e)]. This clearly demonstrates the synergistic effect of MACl and [$\text{C}_2\text{OHmim}][\text{Cin}]$ additives, also achieved with another perovskite composition, the triple-cation double-anion $(\text{FA}_{0.98}\text{MA}_{0.02})_{0.95}\text{Cs}_{0.05}\text{Pb}(\text{I}_{0.98}\text{Br}_{0.02})_3$ perovskite [Figure 1(f)–(h)].

It is noteworthy that this effect is also observed in the X-ray diffraction (XRD) patterns of the obtained films. Whereas the diffraction patterns for the reference $\text{FA}_{0.85}\text{Cs}_{0.15}\text{PbI}_3$ films and the samples with 1% of [$\text{C}_2\text{OHmim}][\text{Cin}]$ or 15% of MACl remain the same, the diffraction pattern of the film containing both 1% of [$\text{C}_2\text{OHmim}][\text{Cin}]$ and 15% of MACl shows, all other things being equal, a much higher intensity of reflections and a preferential orientation of grains along the [100] crystallographic direction [Figure 2(a)]. The effect of MACl on the preferential orientation of perovskite was previously reported for MAPbI_3

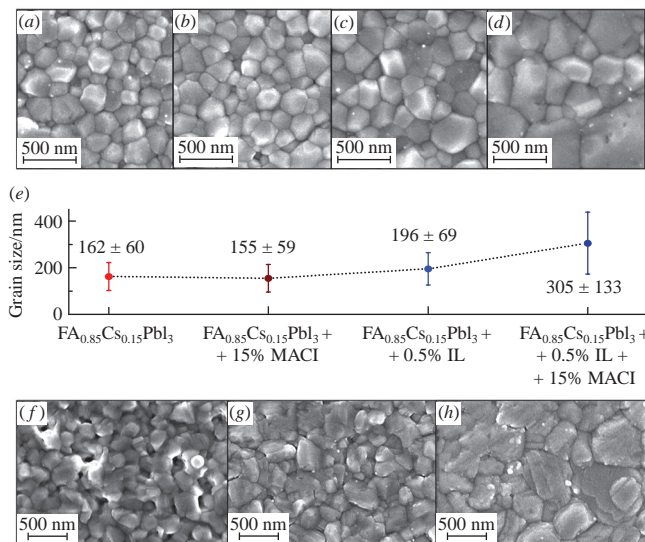


Figure 1 (a)–(d) SEM images of (a) the reference $\text{FA}_{0.85}\text{Cs}_{0.15}\text{PbI}_3$ film and $\text{FA}_{0.85}\text{Cs}_{0.15}\text{PbI}_3$ films with additives of (b) 15% MACl , (c) 0.5% IL and (d) 15% MACl + 0.5% IL. (e) Average grain sizes of the $\text{FA}_{0.85}\text{Cs}_{0.15}\text{PbI}_3$ films with and without additives. (f)–(h) SEM images of (f) the reference $(\text{FA}_{0.98}\text{MA}_{0.02})_{0.95}\text{Cs}_{0.05}\text{Pb}(\text{I}_{0.98}\text{Br}_{0.02})_3 + 15\% \text{ MACl}$ film and films of the same composition with additional additives of (g) 0.5% IL and (h) 1% IL.

[†] For details, see Online Supplementary Materials.

and was attributed to the formation of highly oriented, due to the presence of MACl , intermediate phases such as $\text{MA}_2(\text{DMF})_2\text{Pb}_3\text{I}_8$.^{21,30}

MACl has a ‘soft’ lattice and is considered to be an ionic plastic crystal with fast translational self-diffusion.³¹ As a result, components easily penetrate through and into the soft lattice of the hybrid perovskite,³² forming intermediates during crystallization and annealing at high temperature.^{20,30} Upon further annealing of the film, MACl completely leaves the film (within a few minutes at 150 °C).²⁰ We hypothesize that the simultaneous addition of IL and MACl facilitates the formation of MACl -based intermediates and hinders their transformation, which leads to a decrease in the perovskite crystallization rate and the observed formation of larger grains as a consequence.

Interestingly, despite the similarity of morphological changes in $\text{FA}_{0.85}\text{Cs}_{0.15}\text{PbI}_3$ and $(\text{FA}_{0.98}\text{MA}_{0.02})_{0.95}\text{Cs}_{0.05}\text{Pb}(\text{I}_{0.98}\text{Br}_{0.02})_3$ perovskite films, the PL spectroscopy data reveal some differences. For the triple-cation double-anion $(\text{FA}_{0.98}\text{MA}_{0.02})_{0.95}\text{Cs}_{0.05}\text{Pb}(\text{I}_{0.98}\text{Br}_{0.02})_3$ perovskite films with both additives (IL + MACl), a 73% increase in PL intensity is observed [Figure 2(d)] along with a decrease in the FWHM of the emission peak from 44.5 to 41.5 nm [Figure 2(e)], while the center of the PL peak is blue shifted by 2–3 nm [Figure 2(f)]. These changes indicate a reduced defect density due to a decrease in the number of nonradiative recombination centers in the perovskite material.²⁰ This may also correspond to an improvement in the texture of the perovskite film, which typically reduces the nonradiative recombination experimentally observed in the case of simultaneous IL + MACl passivation.³³

For $\text{FA}_{0.85}\text{Cs}_{0.15}\text{PbI}_3$ films, the FWHM values and peak position changes are the same as those of triple-cation perovskite films with the co-addition of IL and MACl [Figure 2(e), (f)]. However, the PL intensity of $\text{FA}_{0.85}\text{Cs}_{0.15}\text{PbI}_3$ films is slightly reduced compared to the reference films [Figure 2(d)]. Therefore, the optoelectronic properties of the perovskite with the composition of $(\text{FA}_{0.98}\text{MA}_{0.02})_{0.95}\text{Cs}_{0.05}\text{Pb}(\text{I}_{0.98}\text{Br}_{0.02})_3$ appear to be more sensitive to this passivation strategy. Hence, the triple-cation composition was chosen for the further fabrication of PSCs to evaluate the effect of passivation on the performance and stability of the devices. The IL concentration of 0.5% seems to be sufficient to improve both the optoelectronic properties of the perovskite and its microstructure.

It is important to note that the passivated perovskite films of the composition $(\text{FA}_{0.98}\text{MA}_{0.02})_{0.95}\text{Cs}_{0.05}\text{Pb}(\text{I}_{0.98}\text{Br}_{0.02})_3$ also exhibit improved photooxidative stability to visible light under ambient air conditions compared to the $\text{FA}_{0.85}\text{Cs}_{0.15}\text{PbI}_3$ films. While the reference $(\text{FA}_{0.98}\text{MA}_{0.02})_{0.95}\text{Cs}_{0.05}\text{Pb}(\text{I}_{0.98}\text{Br}_{0.02})_3$ films turned yellow after 170 h of exposure to 1 sun illumination under ambient air conditions due to the formation of PbI_2 upon photooxidative decomposition of perovskite,³⁴ the films with 0.5 and 1% of [$\text{C}_2\text{OHmim}][\text{Cin}]$ together with 15% of MACl still remained brownish.

To investigate the synergistic effect of [$\text{C}_2\text{OHmim}][\text{Cin}]$ and MACl on the *operando* parameters of the devices based on the passivated films, solar cells with an inverted planar architecture ITO/PTAA/ MgF_2 / $(\text{FA}_{0.98}\text{MA}_{0.02})_{0.95}\text{Cs}_{0.05}\text{Pb}(\text{I}_{0.98}\text{Br}_{0.02})_3/\text{C}_60$ /BCP/Cu were fabricated [Figure 3(a), †].³⁵ MgF_2 is used as an interface layer between the PTAA and perovskite layers and also as a capping layer on the top of the devices to encapsulate the PSCs as described by Belich *et al.*³⁶ The *J–V* curves of the fabricated devices[†] [Figure 3(b)–(e)] showed that due to the smaller J_{sc} and FF, the PSCs with [$\text{C}_2\text{OHmim}][\text{Cin}]$ and MACl have a lower average initial PCE of 13.2% compared to the reference device with a PCE of 15.1% [see Figure 3(b)]. However, long-term photothermal stability testing of the

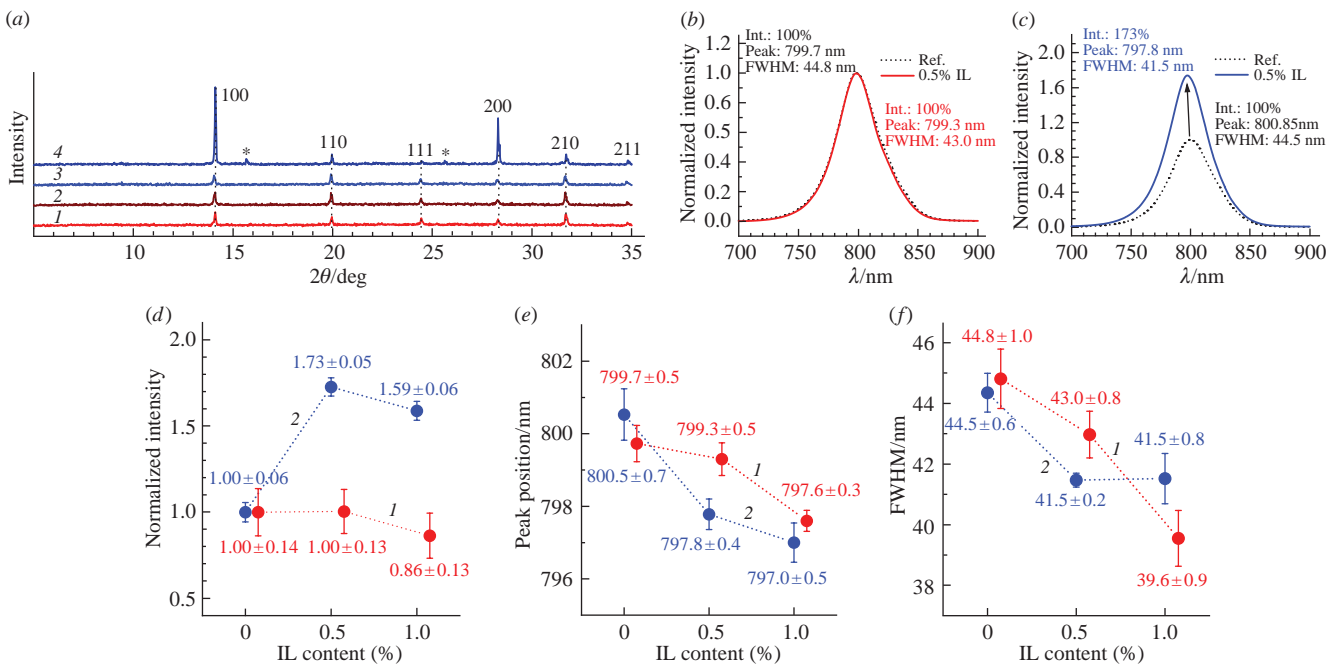


Figure 2 (a) XRD patterns of (1) the reference $\text{FA}_{0.85}\text{Cs}_{0.15}\text{PbI}_3$ film and $\text{FA}_{0.85}\text{Cs}_{0.15}\text{PbI}_3$ films with additives of (2) 15% MACl, (3) 1% IL and (4) 1% IL + 15% MACl (the asterisk '*' indicates an unknown impurity phase). (b), (c) PL spectra of (b) $\text{FA}_{0.85}\text{Cs}_{0.15}\text{PbI}_3$ + 15% MACl and (c) $(\text{FA}_{0.98}\text{MA}_{0.02})_{0.95}\text{Cs}_{0.05}\text{Pb}(\text{I}_{0.98}\text{Br}_{0.02})_3$ + 15% MACl films with (solid line) and without (dotted line) the additive of 0.5% IL. (d)–(f) Dependences of (d) the PL peak intensity (normalized relative to the reference sample), (e) PL peak position and (f) PL peak FWHM of (1) $\text{FA}_{0.85}\text{Cs}_{0.15}\text{PbI}_3$ + 15% MACl and (2) $(\text{FA}_{0.98}\text{MA}_{0.02})_{0.95}\text{Cs}_{0.05}\text{Pb}(\text{I}_{0.98}\text{Br}_{0.02})_3$ + 15% MACl films on the content of IL additive.

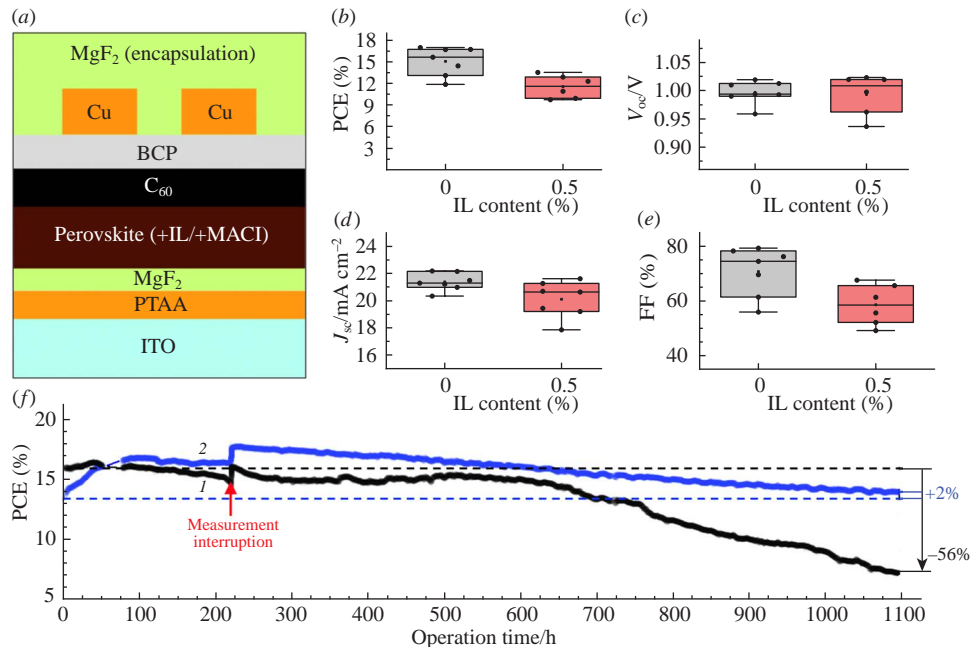


Figure 3 (a) Structure of the fabricated devices, where BCP, PTAA and ITO stand for bathocuproine, poly[bis(4-phenyl)(2,4,6-trimethylphenyl)amine] and indium tin oxide coated glass, respectively. (b)–(e) PCE, V_{oc} , J_{sc} and FF values of the fabricated devices. (f) Continuous MPPT tests for (1) the reference device and (2) the device with 0.5% of $[\text{C}_2\text{OHmim}][\text{Cin}]$ and 15% of MACl.

encapsulated devices, performed using continuous maximum power point tracking (MPPT) under constant 1 sun illumination ($100 \pm 10 \text{ mW cm}^{-2}$) in ambient air at $\sim 55^\circ\text{C}$,[‡] demonstrated the superior stability of the passivated devices [Figure 3(f)]. The efficiency of these devices increased steadily during the first 100 h of measurement, outperforming the reference device and reaching a PCE of almost 17%. Such an increase in PCE has been reported many times in the literature^{37,38} and could be caused by one or more ongoing light-induced processes in the perovskite solar cell, such as annihilation of point defects in the perovskite film,³⁹ improvement of interfaces⁴⁰ and further interaction between the perovskite and the IL. The next part of

the stability test demonstrates a very slow decrease in the PCE of the passivated PSCs with a resulting change of +2% from the initial PCE value. The reference PSC demonstrates -56% of the initial PCE at the end of the experiment.

In conclusion, IL 1-(2-hydroxyethyl)-3-methyl-1*H*-imidazol-3-ium cinnamate was shown to be an effective passivation agent when co-applied with MACl. For FA-based mixed-cation perovskite films with different compositions, co-passivation with IL + MACl leads to an increase in perovskite grain size and PL intensity along with a decrease in the FWHM of the emission line, indicating a reduction of the defect density in the perovskite material. Such a synergistic effect of IL and MACl ultimately

improved the photothermal stability of PSCs and enabled the initial PCE to be fully retained, while the reference device lost 56% of PCE within 1100 h of light soaking.

This work was supported by the Russian Science Foundation (grant no. 22-73-00286). XRD and SEM studies were performed using the equipment of the Joint Research Center for Physical Methods of Research of the N. S. Kurnakov Institute of General and Inorganic Chemistry of the Russian Academy of Sciences (JRC PMR IGIC RAS). The authors thank Anna V. Vavina, Marina M. Seitkalieva and Valentin P. Ananikov from the N. D. Zelinsky Institute of Organic Chemistry for providing the ionic liquid $[C_2OHmim][Cin]$ for the experiments.

Online Supplementary Materials

Supplementary data associated with this article can be found in the online version at doi: 10.1016/j.mencom.2024.10.023.

References

- [dataset] NREL, *Best Research-Cell Efficiency Chart*, 2024; <https://www.nrel.gov/pv/cell-efficiency.html>.
- H. Zhu, S. Teale, M. N. Lintangpradip, S. Mahesh, B. Chen, M. D. McGehee, E. H. Sargent and O. M. Bakr, *Nat. Rev. Mater.*, 2023, **8**, 569; <https://doi.org/10.1038/s41578-023-00582-w>.
- N. N. Udalova, N. N. Chertorizhskiy, E. N. Nemygina, A. V. Trubnikov, A. V. Kurkin, E. A. Goodilin and A. B. Tarasov, *Mendeleev Commun.*, 2023, **33**, 679; <https://doi.org/10.1016/j.mencom.2023.09.028>.
- Z. Wu, E. Bi, L. K. Ono, D. Li, O. M. Bakr, Y. Yan and Y. Qi, *Nano Energy*, 2023, **115**, 108731; <https://doi.org/10.1016/j.nanoen.2023.108731>.
- X. Deng, L. Xie, S. Wang, C. Li, A. Wang, Y. Yuan, Z. Cao, T. Li, L. Ding and F. Hao, *Chem. Eng. J.*, 2020, **398**, 125594; <https://doi.org/10.1016/j.cej.2020.125594>.
- Md. Shahiduzzaman, E. Y. Muslih, A. K. M. Hasan, L. Wang, S. Fukaya, M. Nakano, M. Karakawa, K. Takahashi, Md. Akhtaruzzaman, J.-M. Nunzi and T. Taima, *Chem. Eng. J.*, 2021, **411**, 128461; <https://doi.org/10.1016/j.cej.2021.128461>.
- J. Luo, F. Lin, J. Yuan, Z. Wan and C. Jia, *ACS Mater. Lett.*, 2022, **4**, 1684; <https://doi.org/10.1021/acsmaterialslett.2c00091>.
- J. Yang, J. Hu, W. Zhang, H. Han, Y. Chen and Y. Hu, *J. Energy Chem.*, 2023, **77**, 157; <https://doi.org/10.1016/j.jechem.2022.10.048>.
- F. Wang, D. Duan, M. Singh, C. M. Sutter-Fella, H. Lin, L. Li, P. Naumov and H. Hu, *Energy Environ. Mater.*, 2023, **6**, e12435; <https://doi.org/10.1002/eem2.12435>.
- T. Niu, L. Chao, W. Gao, C. Ran, L. Song, Y. Chen, L. Fu and W. Huang, *ACS Energy Lett.*, 2021, **6**, 1453; <https://doi.org/10.1021/acsenergylett.0c02696>.
- S. Maniyarasu, B. F. Spencer, H. Mo, A. S. Walton, A. G. Thomas and W. R. Flavell, *J. Mater. Chem. A*, 2022, **10**, 18206; <https://doi.org/10.1039/d2ta03748c>.
- S. Zhang, T. Xiao, F. Fadaei Tirani, R. Scopelliti, M. K. Nazeeruddin, D. Zhu, P. J. Dyson and Z. Fei, *Inorg. Chem.*, 2022, **61**, 5010; <https://doi.org/10.1021/acs.inorgchem.1c03862>.
- G. Abdelmageed, H. R. Sully, S. Bonabi Naghadeh, A. El-Hag Ali, S. A. Carter and J. Z. Zhang, *ACS Appl. Energy Mater.*, 2018, **1**, 387; <https://doi.org/10.1021/acsaelm.7b00069>.
- M. Li, L. Yu, Y. Zhang, H. Gao, P. Li, R. Chen and W. Huang, *Sol. RRL*, 2020, **4**, 2000481; <https://doi.org/10.1002/solr.202000481>.
- D. Akin Kara, D. Cirak and B. Gultekin, *Phys. Chem. Chem. Phys.*, 2022, **24**, 10384; <https://doi.org/10.1039/D2CP00341D>.
- X. Li, C.-C. Chen, M. Cai, X. Hua, F. Xie, X. Liu, J. Hua, Y.-T. Long, H. Tian and L. Han, *Adv. Energy Mater.*, 2018, **8**, 1800715; <https://doi.org/10.1002/aenm.201800715>.
- L. Guan, N. Jiao and Y. Guo, *J. Phys. Chem. C*, 2019, **123**, 14223; <https://doi.org/10.1021/acs.jpcc.9b02621>.
- F. Wang, D. Duan, Y. Sun, T. Wang, G. Yang, Q. Li, Y. Li, X. Liang, X. Zhou, X. Sun, J. Ma, J. Xiang, J. Zhu, Q. Zhu, K. Zhou, H. Lin, Y. Shi, G. Li and H. Hu, *Nano Energy*, 2024, **125**, 109549; <https://doi.org/10.1016/j.nanoen.2024.109549>.
- S. Liu, Y. Guan, Y. Sheng, Y. Hu, Y. Rong, A. Mei and H. Han, *Adv. Energy Mater.*, 2020, **10**, 1902492; <https://doi.org/10.1002/aenm.201902492>.
- M. Kim, G.-H. Kim, T. K. Lee, I. W. Choi, H. W. Choi, Y. Jo, Y. J. Yoon, J. W. Kim, J. Lee, D. Huh, H. Lee, S. K. Kwak, J. Y. Kim and D. S. Kim, *Joule*, 2019, **3**, 2179; <https://doi.org/10.1016/j.joule.2019.06.014>.
- C. Zhu, C. Wang, P. Zhang, S. Ma, Y. Chen, Y. Zhang, N. Yang, M. Xiao, X. Cheng, Z. Gao, K. Wen, X. Niu, T. Song, Z. Su, H. Zai, N. Li, Z. Huang, Y. Zhang, H. Wang, H. Zhou, F. Xiao, P. Chen, X. Wang, J. Hong, J. Wang, Y. Bai, X. Gao and Q. Chen, *Joule*, 2023, **7**, 2361; <https://doi.org/10.1016/j.joule.2023.08.004>.
- Z. Liu, P. Liu, M. Li, T. He, T. Liu, L. Yu and M. Yuan, *Adv. Energy Mater.*, 2022, **12**, 2200111; <https://doi.org/10.1002/aenm.202200111>.
- A. Alashkar, M. Ayoub, T. Ibrahim, M. Khamis, P. Nancarrow, A. H. Alami and N. Tabet, *Int. J. Thermofluids*, 2023, **20**, 100404; <https://doi.org/10.1016/j.ijtf.2023.100404>.
- Y. Miao, Z. Wang, C. Chen, X. Ding, M. Zhai, L. Liu, Z. Xia, H. Wang and M. Cheng, *Sol. RRL*, 2022, **6**, 2200364; <https://doi.org/10.1002/solr.202200364>.
- J. Chen, J. Song, F. Huang, H. Li, S. Liu, M. Wang and Y. Shen, *J. Phys. Chem. C*, 2017, **121**, 17053; <https://doi.org/10.1021/acs.jpcc.7b03279>.
- E. Smecca, Y. Numata, I. Deretzis, G. Pellegrino, S. Boninelli, T. Miyasaka, A. La Magna and A. Alberti, *Phys. Chem. Chem. Phys.*, 2016, **18**, 13413; <https://doi.org/10.1039/c6cp00721j>.
- B. Charles, M. T. Weller, S. Rieger, L. E. Hatcher, P. F. Henry, J. Feldmann, D. Wolverson and C. C. Wilson, *Chem. Mater.*, 2020, **32**, 2282; <https://doi.org/10.1021/acs.chemmater.9b04032>.
- S.-H. Turren-Cruz, A. Hagfeldt and M. Saliba, *Science*, 2018, **362**, 449; <https://doi.org/10.1126/science.aat3583>.
- Y. Li, T. Zhang, F. Xu, Y. Wang, G. Li, Y. Yang and Y. Zhao, *Crystals*, 2017, **7**, 272; <https://doi.org/10.3390/cryst7090272>.
- S. Takahashi, S. Uchida and H. Segawa, *ACS Omega*, 2023, **8**, 42711; <https://doi.org/10.1021/acsomega.3c05463>.
- M. Tansho, D. Nakamura and R. Ikeda, *J. Chem. Soc., Faraday Trans.*, 1991, **87**, 3255; <https://doi.org/10.1039/f19918703255>.
- S. Kumar, G. Hodes and D. Cahen, *MRS Bull.*, 2020, **45**, 478; <https://doi.org/10.1557/mrs.2020.146>.
- S. Jariwala, H. Sun, G. W. P. Adhyaksa, A. Lof, L. A. Muscarella, B. Ehrler, E. C. Garnett and D. S. Ginger, *Joule*, 2019, **3**, 3048; <https://doi.org/10.1016/j.joule.2019.09.001>.
- N. N. Udalova, S. A. Fateev, E. M. Nemygina, A. Zanetta, G. Grancini, E. A. Goodilin and A. B. Tarasov, *ACS Appl. Mater. Interfaces*, 2022, **14**, 961; <https://doi.org/10.1021/acsami.1c20043>.
- N. A. Belich, A. A. Petrov, P. A. Ivlev, N. N. Udalova, A. A. Pustovalova, E. A. Goodilin and A. B. Tarasov, *J. Energy Chem.*, 2023, **78**, 246; <https://doi.org/10.1016/j.jechem.2022.12.010>.
- P. Fassl, Y. Zakharko, L. M. Falk, K. P. Goetz, F. Paulus, A. D. Taylor, J. Zaumseil and Y. Vaynzof, *J. Mater. Chem. C*, 2019, **7**, 5285; <https://doi.org/10.1039/C8TC05998E>.
- Z. Liu, L. Qiu, L. K. Ono, S. He, Z. Hu, M. Jiang, G. Tong, Z. Wu, Y. Jiang, D.-Y. Son, Y. Dang, S. Kazaoui and Y. Qi, *Nat. Energy*, 2020, **5**, 596; <https://doi.org/10.1038/s41560-020-0653-2>.
- Y.-C. Zhao, W.-K. Zhou, X. Zhou, K.-H. Liu, D.-P. Yu and Q. Zhao, *Light: Sci. Appl.*, 2017, **6**, e16243; <https://doi.org/10.1038/lsa.2016.243>.
- D. Guo, Z. Andaji Garmaroudi, M. Abdi-Jalebi, S. D. Stranks and T. J. Savenije, *ACS Energy Lett.*, 2019, **4**, 2360; <https://doi.org/10.1021/acsenergylett.9b01726>.
- H. Tsai, R. Asadpour, J.-C. Blancon, C. C. Stoumpos, O. Durand, J. W. Strzalka, B. Chen, R. Verduzco, P. M. Ajayan, S. Tretiak, J. Even, M. A. Alam, M. G. Kanatzidis, W. Nie and A. D. Mohite, *Science*, 2018, **360**, 67; <https://doi.org/10.1126/science.aap8671>.

Received: 3rd May 2024; Com. 24/7490